IGSHPA Research Track
Las Vegas, December 6-8, 2022

Field tests and numerical simulation of a novel thermal response test equipment for water wells

Satoshi Tanaka **Hikari Fujii** **Hiroyuki Kosukegawa**
Shunsuke Tsuya

ABSTRACT

The objective of this study is to develop a novel thermal response test (TRT) equipment that can be applied to existing water wells instead of borehole heat exchangers (BHEs). Accordingly, field tests were conducted using new and conventional equipment to estimate the vertical distribution of ground thermal conductivity. The result showed that the estimated thermal conductivity profile was higher than the reference profile obtained using conventional equipment. The temperature behavior in the well was considered to be unstable due to natural convection because the heating time was 4 hours, which is not long enough. Next, a numerical model of the water well including the novel equipment was developed, and the model was validated through history matching by using the temperature change in each depth. Finally, the TRT was simulated for two days using the model, and the simulated thermal conductivity profile was similar to the reference profile except near the end of the heated section. This result indicates that a more accurate thermal conductivity profile can be obtained by increasing the heating time until approximately 1.5 days.

INTRODUCTION

The installation of a ground source heat pump (GSHP) system requires drilling a borehole heat exchanger (BHE) to extract and inject heat from and to the ground. However, drilling costs associated with a BHE are higher in Japan than those in other countries because of complex geological structures. The high drilling cost is one of the factors hindering the widespread use of GSHP systems. Therefore, optimizing the length and number of BHEs is important for minimizing the drilling costs. A thermal response test (TRT) is necessary for estimating the thermal properties of the ground and the heat exchange capacity of the BHEs. However, the conventional TRT is conducted using a BHE, which requires drilling of BHEs in the preliminary investigation phase, thus resulting in high costs and operation times.

The objective of this research is to develop a novel TRT equipment that can be applied to existing water wells instead of BHEs for estimating the vertical distribution of thermal conductivities. TRTs using existing water wells can be implemented at lower costs and in a shorter time than the conventional TRT using BHE, as no new wells need to be drilled. If the validity of the proposed equipment can be demonstrated, it can be used to implement TRTs in several wells in Japan, such as pumping wells, re-injection wells, snowmelt wells, and observation wells. In addition, the potential map of the GSHP system is expected to become more sophisticated owing to a significant increase in the number of wells capable of performing TRTs.

Satoshi Tanaka (m6022220@s.akita-u.ac.jp) is a master course student, Hikari Fujii is a professor, Kosukegawa Hiroyuki is a chief engineer, and all at the graduate school of international resource sciences at Akita University. Shunsuke Tsuya is an assistant section chief, Development Department Zeneral Heatpump Industry Co., Ltd.

DOI: https://doi.org/10.22488/okstate.22.000022

We reviewed research about TRTs for estimating the distribution of thermal conductivities. Fujii et al. (2006) conducted TRTs using optical fiber thermometers in two types of BHEs and estimated the distribution of thermal conductivities of the ground using a nonlinear regression method. Moreover, Fujii et al. (2009) estimated the distribution of thermal conductivities using the optical fiber sensors inserted into the U-tubes and indicated the reliability of the optical fiber and interpretation method by consistent estimated distribution with the measured one. Raymond et al. (2015) installed ten short heating cables in the pipe of the heat exchanger to inject heat and estimate the distribution of subsurface thermal conductivity. Isabel et al. (2018) conducted distributed thermal response tests (DTRT) using a heating cable and a fiber optic temperature sensor and attempted to obtain the thermal conductivity distribution. Zhang et al. (2020) conducted an actively heated fiber optics based TRT (ATRT) and obtained a reliable thermal conductivity distribution through comparison with the results of a conventional TRT. A type of copper mesh heated optical cable was used in the ATRT as a heating source along with a temperature sensing cable. Hakara et al. (2022) presented an enhanced thermal response test (ETRT) using a hybrid cable containing copper wires and fiber optics and determined the vertical distributions of thermal conductivities along the drill hole. Advanced TRTs for estimating the distribution of thermal conductivities were summarized by Wilke et al. (2020). However, TRTs using existing water wells by fixing the heating cable and optical fiber on the casing have not been mentioned so far.

Next, we present a study about TRT using ungrouted BHEs. Fujii et al. (2016) conducted an experimental study to confirm the applicability of a TRT to ungrouted wells. They compared the results of a TRT conducted using an ungrouted BHE saturated with groundwater to those of a TRT conducted using a BHE filled with silica sand. They found good agreement between the interpretation results for both the average and depth-specific thermal conductivities. The results indicate that TRTs using ungrouted BHE with casing inner diameters of up to 100 mm are feasible for estimating the thermal conductivity of the ground. Therefore, TRT can be implemented in small-diameter water wells by inserting a U-tube. However, thus far, no TRT equipment using an optical fiber thermometer has been developed that can be directly applied to a water well of large diameters.

TRT using an ungrouted BHE

First, a TRT was conducted using an ungrouted BHE to obtain the vertical distribution of the ground thermal conductivity as reference data. The test field was located on the Akita University campus in Akita City, northern Japan (Fig. 1(a)). The BHE was 60 m long and had a hole diameter of 230 mm. The BHE is cased with the 150 mm/160 mm ID/OD steel casing. The well screen ranged between 42 to 47.5 m, and the BHE was filled with groundwater below the groundwater level of -5.5 m (Fig. 1(b)). The outer and inner diameters of the U-tubes were 34 mm and 27 mm, respectively. The heating medium in the U-tube was 9% ethylene glycol. The inlet and outlet temperatures of the heating medium were measured using the Pt100.

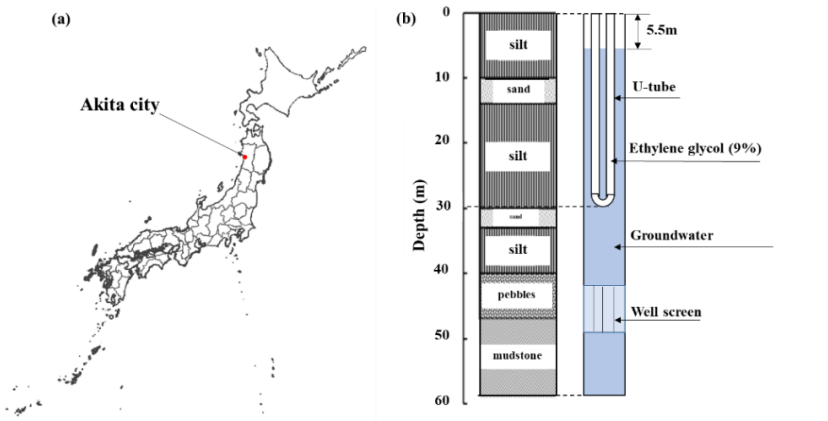

Figure 1 (a) Location of the test field in Japan. (b) Geological columnar section at the test field and overview of the BHE.

The TRT was conducted for 48 h with a circulation rate of 15 L/min and a heating load of 1.5 kW. A fiber-optic thermometer was installed in the U-tube return tube, and the temperature profiles were measured every minute at 0.5 m intervals from the start of the TRT to 72 h after it was completed.

The TRT results are shown in Fig. 2(a). The temperature behavior was temporarily disturbed owing to the reduced heater output during the TRT; however, the heat medium temperature was stable during the entire test period. Figure 2(b) shows the average inlet and outlet temperatures of the heat medium plotted on a semi-logarithmic graph. The apparent thermal conductivity of the ground around the BHE was estimated to be 1.58 W/m/K using the slope method. Additionally, the temperature after the stabilized heater output was used to estimate thermal conductivity. The temperature profiles measured by the optical fiber at each time point are shown in Fig. 3(a). The temperature profiles shown in the figure are at the end of the TRT; 12, 24, 48, and 72 h after the end of the TRT; and before the start of the TRT. Next, we estimated the thermal conductivity profile of the ground using the analysis method proposed by Fujii et al. (2009). This analysis method is based on a nonlinear regression method, and the thermal conductivity profile is estimated by minimizing the evaluation function F defined in equation (1).

$$F = \alpha \sum^{nstep} \left(T_{O(obs)} - T_{o(cal)}\right)^2 + (1-\alpha) \sum^{ntest} \left(\sum^{nlayer} \left(T_{ro(obs)} - T_{ro(cal)}\right)^2 \right) \quad (1)$$

The parameters used for the calculation in Equation (1) are listed in Table 1. Considering the groundwater level, the number of layers was set to 25 (each layer was 1 m thick) because the effective length of the BHE is 25 m. The length and number of time steps were set to 12 min and 240, respectively, corresponding to the period of the TRT. The thermal conductivity profile of the ground around the BHE was estimated using the above-mentioned analysis method (Fig. 3(b)). The average thermal conductivity of the entire ground was 1.51 W/m/K, which was similar to the apparent thermal conductivity of 1.58 W/m/K (Fig. 2(b)). Therefore, the thermal conductivity profile estimated using the analysis method was considered as the reference data.

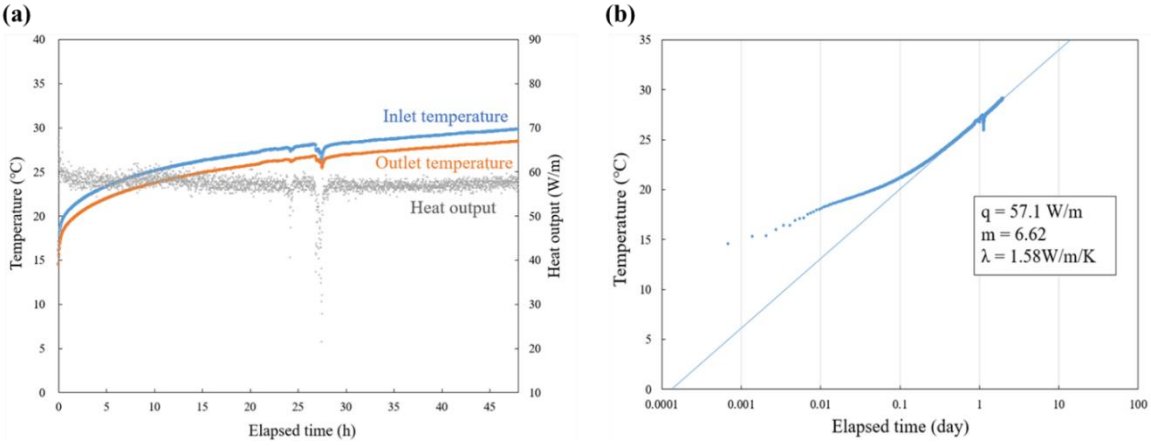

Figure 2 (a) Inlet and outlet temperatures and heat output during the TRT. (b) Change in the average inlet and outlet temperatures of the heat medium.

Table 1. Parameters used in equation (1) to determine the evaluation function

Number of Layers	nlayer	25
Number of calculations	nstep	240
Number of temperature comparisons	ntest	3
Weighting constant	α	0.05

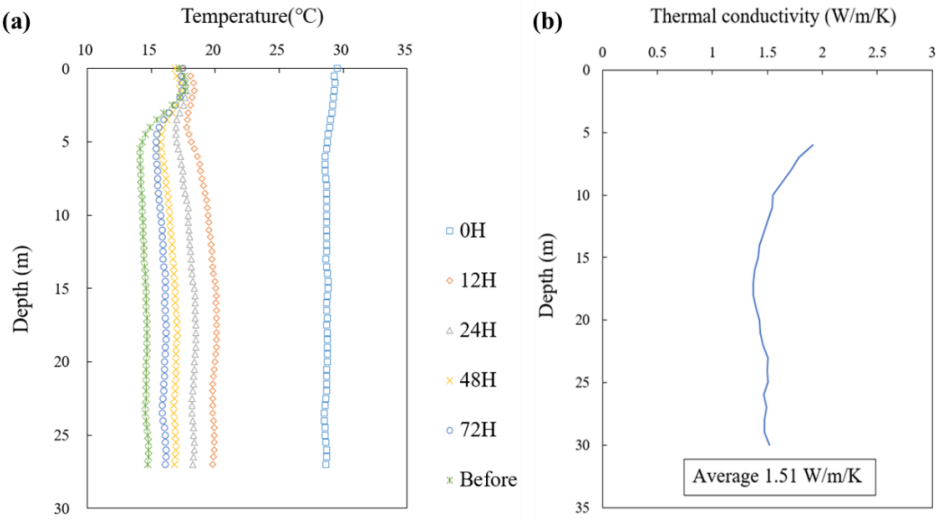

Figure 3 (a) Temperature profiles measured using the optical fiber at each time step. (b) Thermal conductivity profile of the ground around the BHE.

A TRT using the novel TRT equipment

Figure 4(a) shows a photograph of the novel TRT equipment, and Fig. 4(b) shows a schematic of the equipment installation. The equipment was composed of a ground control unit and a measurement cable installed in the water wells. The measurement cable comprised three parts: a waterproof ribbon heater, a fiber optic thermometer, and electromagnet units. Each electromagnet unit is equipped with an electromagnet and integrated on the measurement cable at 2.2 m intervals. The electromagnet in electromagnet unit adheres to the casing by passing an electric current by the control unit. Then, the electromagnet unit draws the heater and optical fiber to the casing. Figure 5(a) shows the main monitor of the control unit, and Fig. 5(b) shows a photograph of the test equipment installed at the field test site. This new equipment was designed to be used in the existing water wells instead of BHEs, and the measurement cable was fixed on the inner wall of the steel casing in the water well via adsorption of the electromagnet units. During the TRT, the ground around the water well was heated using a ribbon heater. Water temperature was measured at 0.5 m intervals using a fiber optic thermometer to estimate the thermal conductivity at each depth using the slope method.

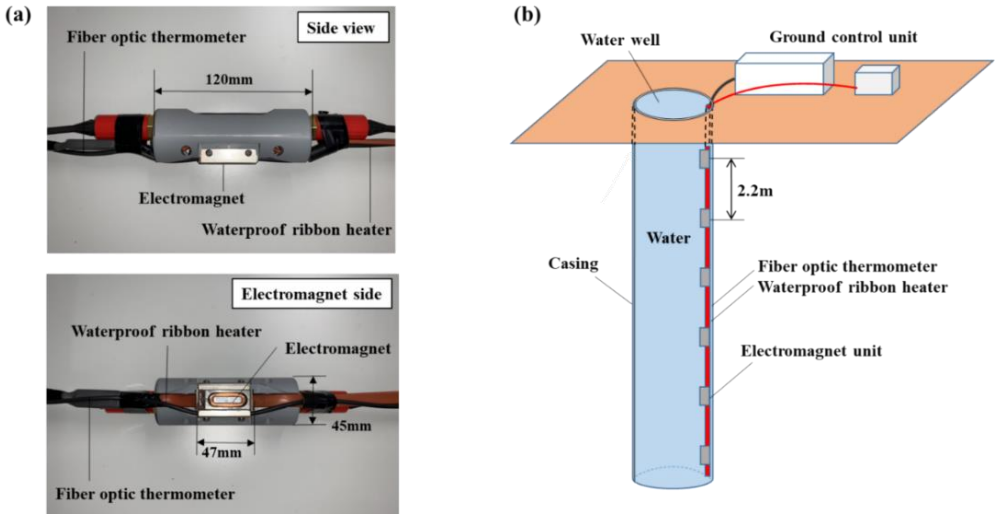

Figure 4 (a) Electromagnet unit of the novel TRT equipment. (b) Schematic of the installation of the novel TRT equipment.

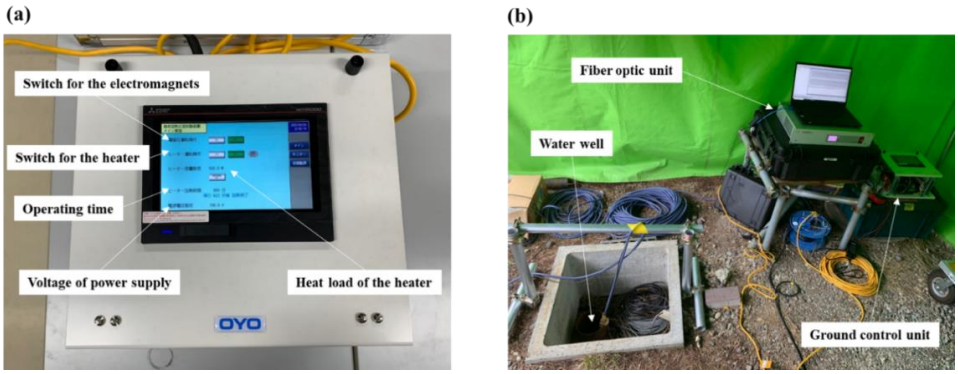

Figure 5 (a) Main monitor of the ground control unit. (b) Installed equipment for conducting the TRT.

A TRT was performed using the new equipment with a test duration of 4 h and a heating load of 50 W/m. The water well used in this TRT was a BHE without a U-tube. The measurement cable was installed in the section located between the 10 m and 20 m depths of the water well. L-shaped supports were used to ensure that each electromagnetic unit faces the inner wall of the casing after the measurement cable was installed. Using an underwater camera, we confirmed that the measurement cable was installed along the inner wall of the casing.

Figure 6(a) shows the measured temperature at each depth during the TRT. To smooth the fluctuation of fiber optic thermometer measurements, the measured temperatures were output as a 5-minute moving average. The results indicated that the temperature increase at both ends of the measurement cable was smaller than that around the central part of the measurement cable. This result is considered to be due to the presence of unheated sections at the top and bottom of the measurement cable, which suppressed the temperature rise. Figure 6(b) compares the thermal conductivity profile estimated using the new TRT equipment and the reference profile shown in Fig. 3(b). The comparison results showed that the estimated thermal conductivity at -16 m (near the center of the heated section) was

the lowest among all depths. In addition, the thermal conductivity increased from a depth of 16 m toward both ends of the measurement cable. Moreover, the thermal conductivities estimated using the TRT equipment were higher than those of the reference profile at all depths. This is considered that the water well was not sufficiently heated because the test time was only 4 h, and the temperature behavior was unstable owing to natural convection. Therefore, to obtain a more accurate thermal conductivity profile, a longer testing time is necessary.

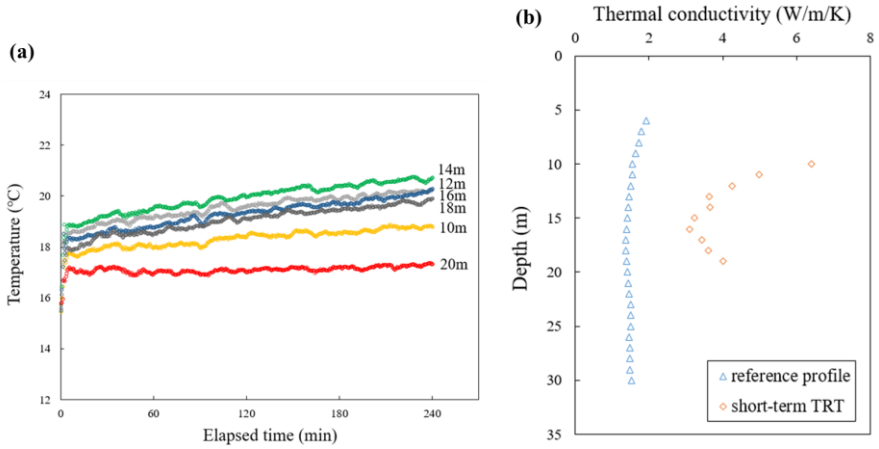

Figure 6 (a) Temperature change at each depth during the TRT. (b) Thermal conductivity profile estimated via the TRT.

Numerical modeling of the TRT using the new equipment

A numerical model including the new TRT equipment, ground, and water well was developed using the finite element subsurface FLOW (FEFLOW) software ver. 7.1 to reproduce the TRT. The developed numerical model is shown in Fig. 7. The radius and height of the model were 3 m and 40 m, respectively. The inner diameter and casing thickness of the water well were set to 0.15 m and 0.005 m, respectively. The number of layers with a thickness of 0.5 m is 60 from the top to -30 m, while two layers with a thickness of 5 m are located between 30 m and 40 m. The thermal conductivity of the ground was input for each layer based on the reference thermal conductivity profile. The thermal conductivity deeper than 30 m and permeability of ground at each layer were determined by referring to the geological column shown in Fig. 1(b). The heat flux of the heater on the casing wall was fixed from -10 to -20 m. The external boundary of the model was adiabatic, and the initial temperature of the model was set at 16.37°C based on the TRT result.

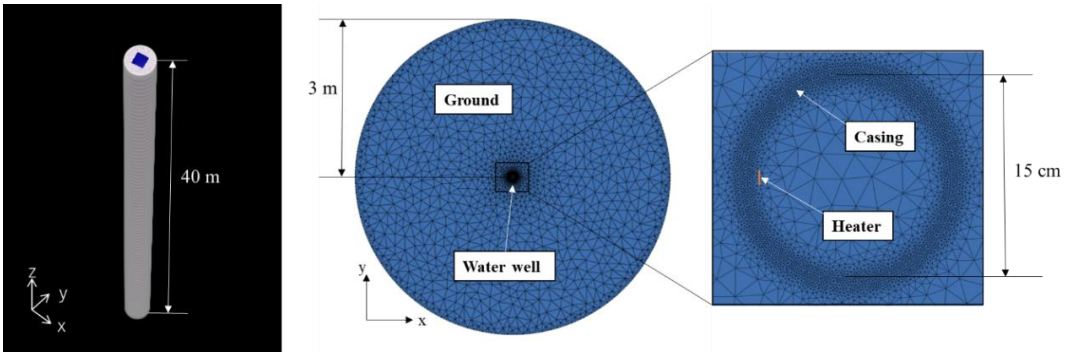

Figure 7 Structure of the numerical model.

To confirm the validity of the numerical model, history matching was performed by using the measured temperature changes at each depth. Figure 8 shows the results of history matching at depths of 14, 15, and 16 m. From the results, the calculated and measured values showed generally good agreement. Therefore, the model is considered valid.

Next, a 2 days TRT simulation was performed using the developed model, and the thermal conductivity profile was estimated from the calculated temperature changes at each depth. Figure 9(a) shows the simulated temperature change at each depth during the simulated TRT. Figure 9(b) shows a comparison between the thermal conductivity profiles estimated using the simulated TRT and reference profiles. To estimate the thermal conductivity, the simulated temperatures from 1 to 1.5 days were used. The results indicated that the thermal conductivity profiles estimated by using the TRT simulation generally agreed with the reference profiles, except near the end of the heated section. Therefore, the TRT equipment developed in this study was considered capable of estimating generally accurate thermal conductivity profiles with a test time of approximately 1.5 days. In the next step of this research, we will perform longer TRTs, while modifying the TRT equipment to estimate a more accurate thermal conductivity profile.

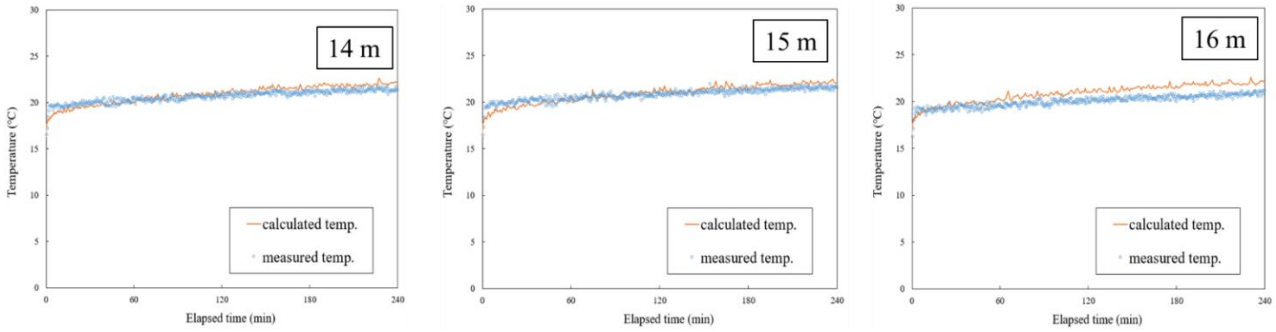

Figure 8 History matchings of water temperature at depths of 14, 15, and 16 m.

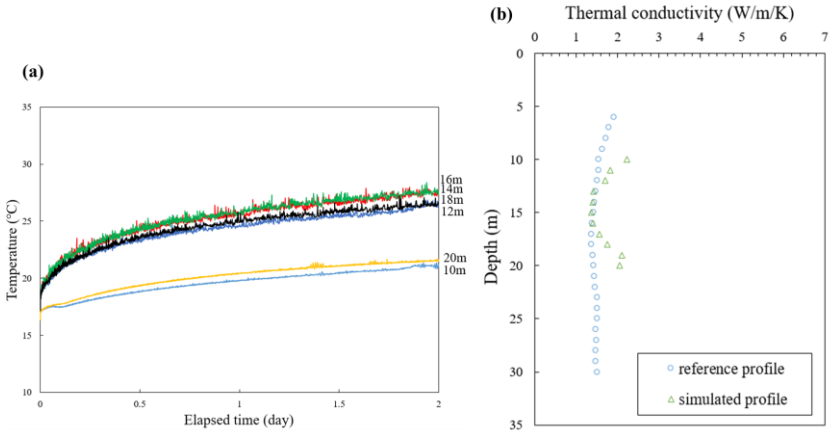

Figure 9 (a) Calculated temperature changes at each depth during the 2 days TRT. (b) Thermal conductivity profile estimated using the result of the TRT simulation.

CONCLUSION

A TRT was conducted using the novel equipment to estimate the thermal conductivity profile. Consequently, the

temperature increase at the end of the heated section was small; however, it augmented toward the center of the heated section. The thermal conductivities estimated using the measured temperatures were greater than those of the reference profile at all depths of the measured section. This is because the test was only conducted for 4 h, during which the temperature behavior in the water well was not stable due to natural convection.

A numerical model including the new TRT equipment was developed using FEFLOW ver. 7.1. To confirm the validity of the numerical model, a numerical simulation reproducing the field test was conducted, and history matching was performed using the TRT result. The measured and calculated temperature changes at each depth showed generally good agreement, and the validity of the model was confirmed. Next, a TRT simulation was performed for two days, and the thermal conductivity profile was estimated using the calculated temperature changes at each depth. The estimated thermal conductivity profile was in good agreement with the reference profiles except near the end of the heated section. Therefore, a sufficient TRT period (approximately 1.5 d) is estimated to stabilize the temperature behavior in the water and realizes accurate thermal conductivity profiles.

ACKNOWLEDGMENTS

This paper is based on results obtained from a project, JPNP19006, subsidized by the New Energy and Industrial Technology Development Organization (NEDO).

NOMENCLATURE

F = Evaluation function (K^2)
α = Wighting constant (−)
T = Temperature (℃)

Subscripts

o = outlet of U-tube
ro = outer wall of a ground heat exchanger
obs = observation
cal = calculation

REFERENCES

Fujii, H., H, Okubo and R, Ito. 2006. *Thermal response tests using optical fiber thermometers.* Geothermal Resources Council 30: 545 -551.

Fujii, H., H, Okubo., K, Nishi., R, Itoi., K, Ohyama and K, Shibata. 2009. *An improved thermal response test for U-tube ground heat exchanger based on optical fiber thermometers*. Geothermics 38: 399-406.

Fujii, H., H, Kosukegawa., H, Farabi and S, J, Nasrabady. 2016. *Experimental study on the applicability of ungrouted ground heat exchangers on thermal response tests*. J.Geotherm. Res. Soc. Japan 28(2): 43-51.

Hakala, P., S, Vallin., T, Arola and I, Martinkauppi. 2022. *Novel use of the enhanced thermal response test in crystalline bedrock*. Renewable Energy 182: 467-482.

Isabel, M., V, Márquez., J, Raymond., D, Blessent., M, Philippe., N, Simon., O, Bour and L, Lamarche. 2018. *Distributed Thermal Response Tests Using a Heating Cable and Fiber Optic Temperature Sensing*. Energies 11: 3059.

Raymond, J., L, Lamarche and M, Malo. 2015. *Field demonstration of a first thermal response test with a low power source*. Applied Energy 147: 30-39.

Wilke, S., K, Menberg., H, Steger and P, Blum. 2020. *Advanced thermal response tests: A review*. Renewable and Sustainable Energy Reviews 119: 109575.

Zhang, B., K, Gu., B, Shi., C, Liu., P, Bayer., G, Wei., X, Gong and L, Yang. 2020. *Actively heated fiber optics based thermal response test: A field demonstration.* Renewable and Sustainable Energy Reviews 134: 110336.